Comparative Analysis between ^{18} F- PSMA-1007 and ^{18}F-FDG PET-CT scans in Metastatic Prostate Carcinoma: A Case Report

[1]Papia Akhter, [2]Md. Abu Bakker Siddique, [3]Pupree Mutsuddy,[1]Tapati Mandal, [4] S. M. Arifur Rahman, [5]A.K.M Fazlul Bari

[1]Assistant Professor, [2]Professor & Head, PET-CT Division, [3]Associate Professor, [4]Medical Officer, [5]Professor & Director
National Institute of Nuclear Medicine & Allied Sciences (NINMAS)

Correspondence Address: Dr Papia Akhter, Assistant Professor, NINMAS, Block-D, BMU Campus, Dhaka-1000. Email: papia1078@gmail.com

ABSTRACT

Background: Prostate cancer is the second leading cause of cancer death in males and has a poor prognosis if present with metastasis. Proper management demands precise and reliable detection of the extent of disease, finally staging where molecular imaging plays the crucial role. The ^{18}F PSMA-1007 PET-CT scan is more specific for the detection of prostate cancer. An ^{18}F-FDG scan may be positive in prostate cancer when the tumor uses glucose metabolism or due to upregulation of glucose transporter-1. So, in case of aggressive or dedifferentiated prostate carcinoma, ^{18}F-FDG PET-CT may provide precise localization of metastases.

Case Report: A 78-year-old man with a history of hematuria consulted a physician, and after proper evaluation, he was diagnosed with a case of prostate cancer five years back. Transurethral resection of the prostate was done. During this interval period, the patient was not in follow-up, and no chemotherapy or radiotherapy was given. A follow-up ultrasound showed an enlarged prostate with heterogeneous parenchyma, and a biopsy from the prostate revealed adenocarcinoma (Gleason's score 7-grade group 3) with a high serum PSA level of 52.06 ng/ml. This patient was referred to NINMAS for ^{18}F-PSMA-1007 PET-CT scan to detect recurrence. The PSMA scan demonstrated local recurrence and metastases involving the lungs, liver, skeletal system, and lymph nodes. For academic purposes, a complementary ^{18}F-FDG PET-CT scan was performed, which revealed more detailed information regarding the metastatic lesions, with higher FDG uptake (SUVmax) compared to PSMA uptake. Additionally, the FDG scan provided clearer delineation of hepatic metastases, which were less distinct on the PSMA scan due to the high physiological uptake of PSMA in the liver.

Conclusion: These comparative imaging findings highlight the potential utility of ^{18}F-FDG PET-CT in cases of atypical, aggressive, and dedifferentiated prostate cancer, providing complementary diagnostic insights beyond ^{18}F-PSMA-1007 PET-CT.

Keywords: Prostate carcinoma; PET-CT; ^{18}F-PSMA-1007; ^{18}F-FDG; metastasis.

Bangladesh J. Nucl. Med. Vol. 29 No. 1 January 2026

DOI: https://doi.org/10.3329/bjnm.v29i1.89299

INTRODUCTION

Prostate cancer represents one of the most prevalent malignancies among men worldwide. According to GLOBOCAN 2020, it accounted for an estimated 1,414,000 new diagnoses and 375,304 deaths globally, making it the second most common cancer and the fifth leading cause of cancer mortality in males (1). In Bangladesh, the WHO recorded 1,664 prostate cancer deaths in 2020 (2). While prostate cancer is characteristically slow-growing, a significant subset of patients progresses to advanced or metastatic disease—at which stage the five-year relative survival rate falls to approximately 28%, substantially lower than that of organ-confined or regionally contained disease (3).

Metastatic prostate carcinoma (mPCa) occurs when tumor cells disseminate beyond the confines of the prostate gland, most commonly seeding the regional lymph nodes and axial skeleton, though visceral organs including the lungs and liver may be involved in advanced-stage or castration-resistant disease (3). Precise delineation of the extent of metastatic spread is critical for accurate staging, prognostication, selection of systemic therapy, and the identification of candidates for targeted radionuclide treatments (4, 5).

Molecular imaging via positron emission tomography/computed tomography (PET-CT) currently occupies a central role in the evaluation of prostate cancer. Among the dedicated non-FDG PET tracers, PSMA-targeted ligands, including 68Ga-PSMA-11 and ^{18}F-PSMA-1007, have emerged as the preferred agents for detection, staging, and restaging of prostate cancer (6, 7). PSMA is a type II transmembrane glycoprotein markedly

overexpressed on prostate cancer cells, with expression levels correlating with tumor grade, metastatic potential, and androgen independence (7). ^{18}F-PSMA-1007 offers practical advantages over 68Ga-labeled agents, including a longer half-life, cyclotron-independent supply chain, and critically low urinary excretion, which reduces confounding bladder activity and improves pelvic lesion visualization (8).

18F-fluorodeoxyglucose (FDG) PET-CT, the workhorse of oncological nuclear medicine, exploits the Warburg effect, the preferential utilization of aerobic glycolysis by malignant cells, to detect and characterize tumor deposits (9). Historically, ^{18}F-FDG PET-CT has not been routinely recommended for prostate cancer given the inherently low glycolytic activity of most well-differentiated prostatic adenocarcinoma cells (10). However, in advanced, aggressive, castration-resistant, or phenotypically dedifferentiated prostate carcinoma including tumors exhibiting neuroendocrine differentiation, glucose transporter-1 (GLUT-1) is upregulated, resulting in increased FDG avidity (10,11). In these contexts, ^{18}F -FDG PET-CT may identify lesions displaying a discordant uptake pattern relative to PSMA, so-called 'PSMA-FDG mismatch,' signaling phenotypic plasticity or progression towards a more aggressive biological state (12).

The objective of this case report is to describe and compare the findings of ^{18}F -PSMA-1007 PET-CT and ^{18}F-FDG PET-CT in a patient with extensively metastatic prostate adenocarcinoma and to illustrate how the complementary use of both tracers provides a more comprehensive and biologically nuanced characterization of tumor distribution and behavior than either modality employed in isolation.

CASE REPORT

A 78-year-old Bangladeshi male initially presented to a physician in 2020 with hematuria. Following comprehensive clinical evaluation, he was diagnosed with carcinoma of the prostate. Trans-urethral resection of the prostate (TURP) was performed in 2020 as part of his initial surgical management.

Following TURP, the patient was lost to follow-up and received no adjuvant chemotherapy, external beam radiotherapy, or androgen deprivation therapy (ADT) between 2020 and 2024. This absence of systemic oncological management during a critical therapeutic window represents a clinically significant factor that likely contributed to uninhibited disease progression and the extent of metastatic dissemination observed at re-presentation.

The patient became symptomatic again in 2024. Follow-up ultrasonography (USG) of the pelvis revealed an enlarged prostate gland with heterogeneous parenchymal echotexture—radiologically consistent with disease recurrence. Subsequent transrectal biopsy confirmed prostate adenocarcinoma with a Gleason score of 7 (Grade Group 3), indicating intermediate-to-high risk disease with significant metastatic potential. The serum prostate-specific antigen (PSA) level was markedly elevated at 52.06 ng/mL, strongly suggestive of extensive biologically active disease.

Table 1: Clinical Summary of the prostate cancer patient

Parameter	Details
Age / Gender	78 years / Male
Initial Diagnosis Year	2020
Presenting Symptom	Haematuria
Initial Procedure	Trans-urethral resection of prostate (TURP), 2020
Interim Therapy (2020–2024)	Nil; no chemotherapy, radiotherapy, or androgen deprivation therapy administered
Recurrence Year	2024 (symptomatic)
Follow-up USG	Enlarged prostate with heterogeneous parenchyma
Biopsy (2024)	Prostate adenocarcinoma, Gleason score 7 (Grade Group 3)
Serum PSA Level	52.06 ng/mL (markedly elevated)
Referring Institution	National Institute of Nuclear Medicine & Allied Sciences (NINMAS), BMU Campus, Dhaka, Bangladesh

The patient was referred to NINMAS for ^{18}F-PSMA-1007 PET-CT scanning to assess the extent of local recurrence and systemic metastatic disease. For academic purposes and institutional research, a complementary whole-body ^{18}F-FDG PET-CT scan was subsequently performed, enabling a direct comparative analysis of both imaging modalities in the same patient at the same disease time point.

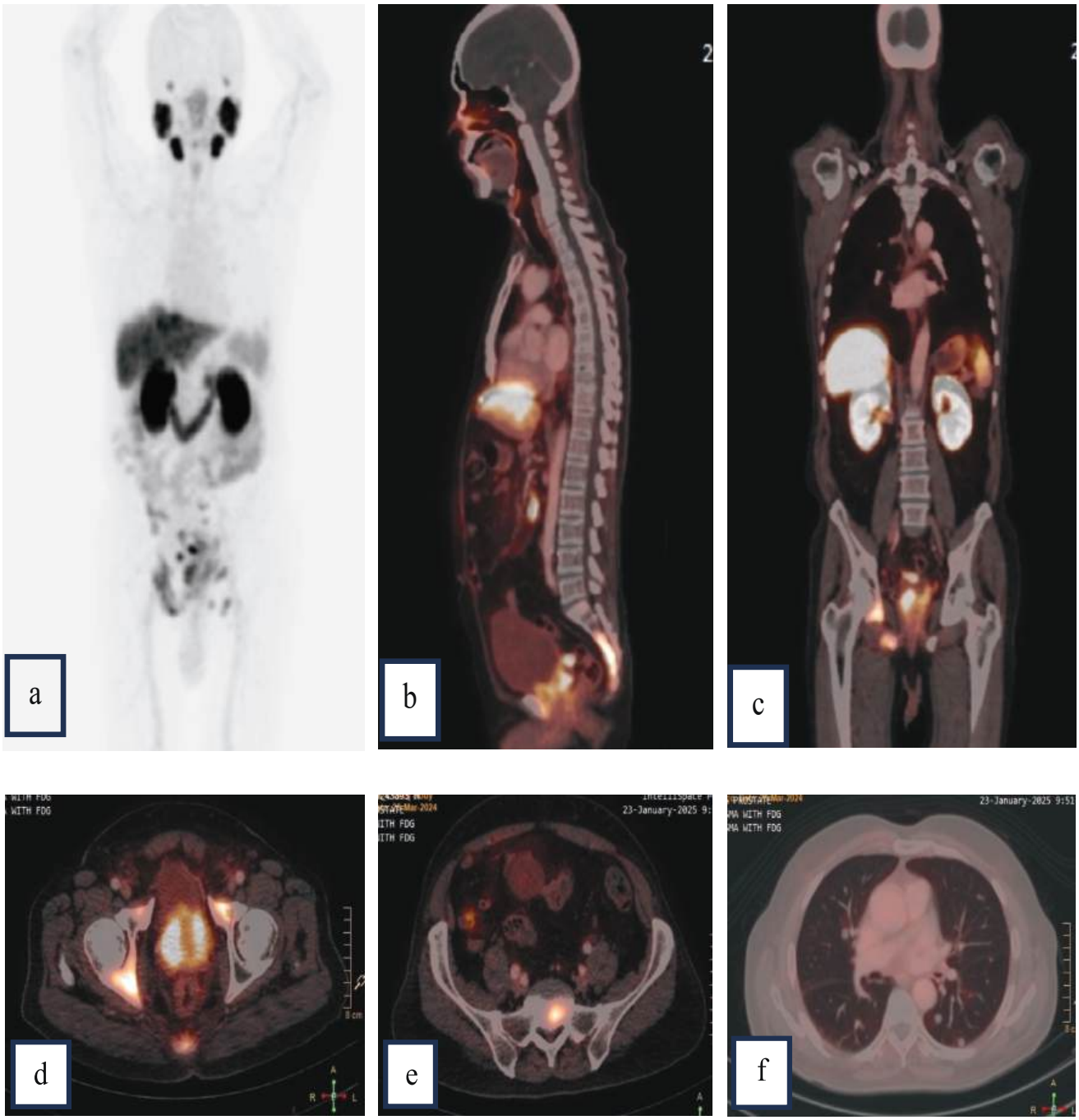

Figure-1:^{18}F PSMA-1009 PET-CT scan of a 78 years old prostate carcinoma patient MIP (a), sagittal (b), coronal (c) and axial (d,e,f) images showing PSMA expression in prostatic tissue suggesting local recurrence (b, c, d), intense PSMA expressing lesion in sacrum, right hip bone suggesting skeletal metastases and low PSMA expressing pulmonary nodules representing pulmonary metastases.

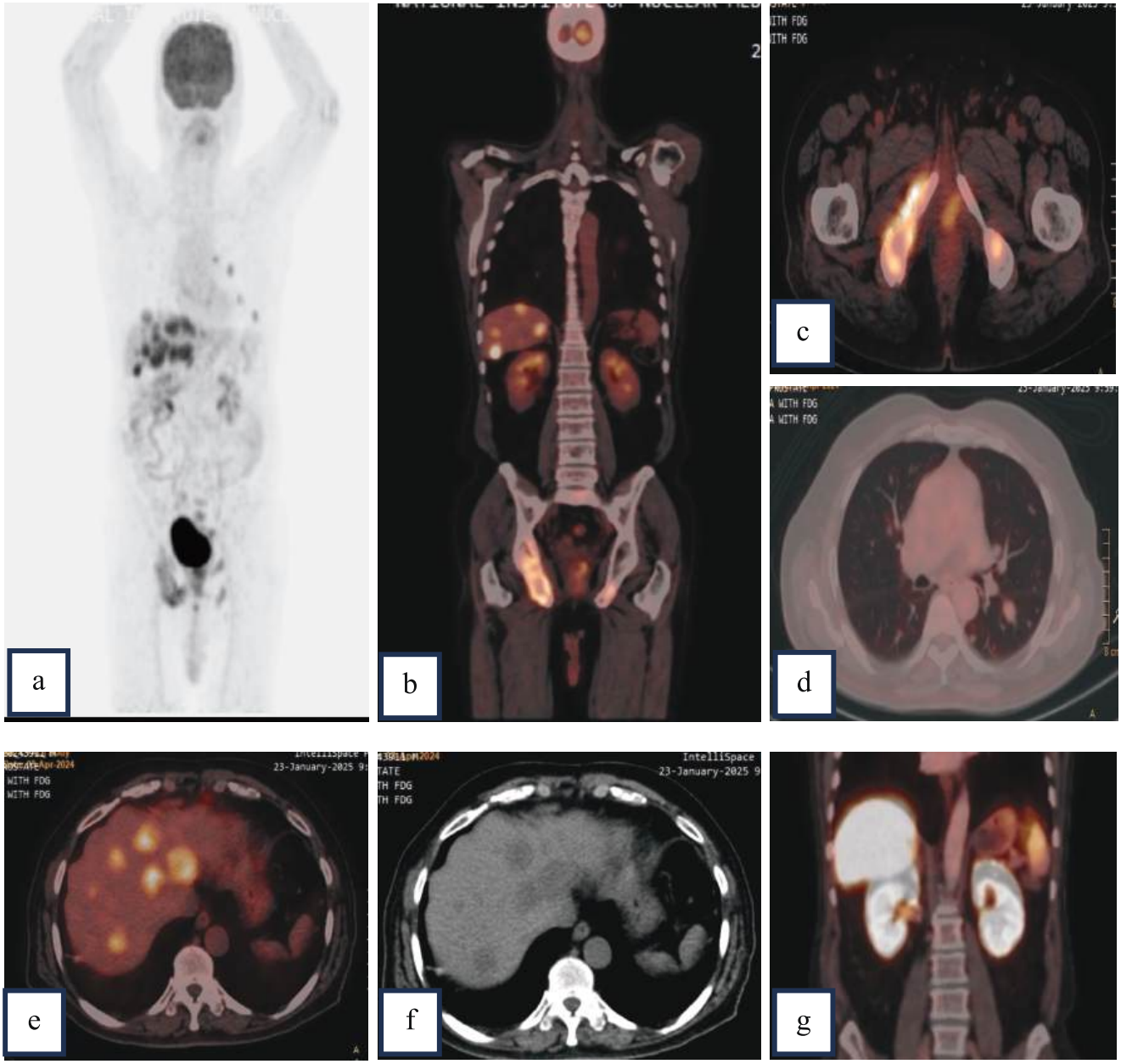

Figure-2: ^{18}F FDG PET CT scan image of the same patient with prostate carcinoma MIP, sagittal and axial images. Images showing along with local recurrence (b), skeletal (b,c) and pulmonary metastases (d) there are multiple FDG avid (e) multiple hypodense SOLs of variable sizes (f) in both lobes of liver which are not well delineated in PSMA PET-CT image (g) due to intense physiological uptake in liver.

DISCUSSION

^{18}F-PSMA-1007 PET-CT Findings

The ^{18}F-PSMA-1007 PET-CT scan demonstrated extensive, multifocal PSMA-avid disease. Local recurrence was confirmed within the prostatic bed, with abnormally elevated radiotracer uptake in residual prostatic tissue —consistent with the clinical presentation of rising PSA and positive re-biopsy (6,13). Multiple skeletal metastases were identified throughout the axial and appendicular skeleton, demonstrating variable but unambiguous PSMA avidity, the expected pattern given the well-characterized osteotropism of prostate cancer (14). PSMA-avid lymphadenopathy was detected across multiple nodal stations, confirming lymph node metastases as part of the systemic tumor burden. Pulmonary lesions with positive PSMA uptake indicated visceral dissemination of disease (6).

Hepatic involvement was noted; however, delineation of hepatic metastases was suboptimal on the PSMA scan. This is attributable to high physiological PSMA expression in normal hepatocytes, which generates an elevated hepatic background signal and reduces lesion-to-background contrast, rendering individual hepatic metastatic deposits comparatively less conspicuous on PSMA imaging (8).

The widespread and intense PSMA avidity across the identified metastatic lesions is clinically important: robust PSMA expression is a prerequisite for eligibility for PSMA-targeted radioligand therapy- specifically Lutetium-177 (177Lu) PSMA therapy- and this patient would potentially satisfy the tracer-uptake criteria for such treatment (4, 5).

^{18}F-FDG PET-CT Findings

The complementary ^{18}F-FDG PET-CT scan yielded several important findings that extended beyond, and in certain anatomical regions meaningfully differed from, the information provided by PSMA imaging (10,12). Across multiple metastatic sites including skeletal lesions, pulmonary deposits, and lymph node metastases the 18F-FDG scan demonstrated elevated maximum standardized uptake values (SUVmax) that were higher than the corresponding PSMA radiotracer uptake in the same lesions. This pattern of FDG-dominance or FDG-PSMA discordance is of considerable biological and prognostic significance (12). It suggests upregulation of glucose metabolism mediated by GLUT-1 overexpression within these tumor deposits, a hallmark of more aggressive, phenotypically altered, or dedifferentiated malignant cells (9,10). In the context of prostate cancer, such findings may indicate transition towards a castration-resistant or neuroendocrine phenotype (15).

The most clinically salient advantage of FDG PET-CT in this case was its superior performance in the delineation of hepatic metastases. Whereas the PSMA scan was limited by high physiological hepatic PSMA uptake, the FDG scan provided markedly improved lesion-to-background contrast in the liver, enabling clear visualization of hepatic metastatic deposits (11). This illustrates a well-described clinical principle: in organs with high physiological PSMA uptake (liver, kidneys, salivary glands, small bowel), FDG may serve as the superior tracer for detecting metastatic disease (8,11).

The concept of 'PSMA-FDG mismatch' wherein lesions show high FDG uptake with relatively lower PSMA expression has been recognized as a marker of aggressive tumor biology, treatment resistance, and potential transition to a PSMA-low or PSMA-negative phenotype (15,12). Although classic mismatch was not the dominant pattern in this case — given preserved PSMA avidity in most lesions the relative FDG predominance in several sites suggests heightened metabolic activity indicative of an aggressive disease course. Patients whose tumours harbour PSMA-negative or PSMA-low metastases may respond sub-optimally to PSMA-directed radioligand therapies and may require additional systemic agents (4,5).

Table 2: Comparative ^{18}F-PSMA-1007 and ^{18}F-FDG PET-CT Findings by Anatomical Region

Anatomical Region	^{18}F-PSMA-1007 PET-CT Findings	^{18}F-FDG PET-CT Findings
Prostate Bed (Local)	PSMA-expressing local recurrence; elevated tracer uptake in residual prostatic tissue	Corresponding FDG-avid uptake confirming local recurrence with elevated glycolytic activity
Skeletal System	Multiple PSMA expressing osseous lesions	FDG-avid osseous lesions; SUVmax exceeds corresponding PSMA uptake in several sites
Lymph Nodes	PSMA expressing distant lymph node metastases	FDG-avid nodal disease; higher glycolytic activity in select nodal groups
Lungs	PSMA-positive pulmonary lesions consistent with parenchymal metastases	FDG-positive pulmonary metastases with elevated SUVmax
Liver	Hepatic involvement less distinct due to high physiological PSMA uptake in normal liver parenchyma	Hepatic metastases more clearly delineated; superior lesion-to-background contrast

Clinical and Pathophysiological Correlation

The comparative imaging findings must be interpreted in the context of the patient's clinical trajectory. The absence of systemic therapy over four years following TURP likely permitted uninhibited tumor progression and the emergence of more aggressive clonal populations. The Gleason score of 7 (Grade Group 3), while classified as intermediate risk at initial diagnosis, is associated with a meaningful probability of extracapsular extension, lymph node involvement, and distant metastasis, particularly in the setting of delayed or absent systemic treatment (3,16).

From a mechanistic perspective, the elevated FDG uptake observed across metastatic lesions reflects increased aerobic glycolysis mediated by upregulated GLUT-1 expression a process driven by hypoxia-inducible factors, oncogene activation, and PI3K/AKT/mTOR pathway dysregulation (9). This metabolic reprogramming is characteristic of aggressive, proliferating tumor cells and correlates with higher histological grade, increased mitotic activity, and poorer prognosis (9,10). The co-existence of robust PSMA avidity with elevated FDG uptake suggests a biologically heterogeneous tumor population potentially comprising both classical androgen-driven, PSMA-expressing cells and more metabolically active, dedifferentiated subclones (15,12).

CONCLUSION

This case report provides a compelling illustration of the complementary diagnostic value of 18F-PSMA-1007 and 18F-FDG PET-CT imaging in a patient with extensively metastatic prostate carcinoma. The 18F-PSMA-1007 PET-CT scan effectively mapped the systemic burden of PSMA-expressing metastatic disease while complementary 18F-FDG PET-CT scan added critical biological information including aggressive metabolic nature of the disease through elevated SUVmax values in multiple lesions and provided superior hepatic lesion delineation, directly overcoming the physiological limitation of high hepatic PSMA background uptake which is a known pitfall of 18F-PSMA-1007 imaging. When used in combination, they provide a uniquely complete portrait of tumor biology integrating spatial distribution, receptor phenotype, and metabolic aggressiveness that neither can achieve in isolation.

CONFLICT OF INTEREST

Authors have no financial, personal, or professional conflicts that could inappropriately bias this work.

REFERENCES

1. Sung H, Ferlay J, Siegel RL, Laversanne M, Soerjomataram I, Jemal A, et al. Global cancer statistics 2020: GLOBOCAN estimates of incidence and mortality worldwide for 36 cancers in 185 countries. CA Cancer J Clin. 2021;71(3):209–49.
2. World Health Organization. Global health estimates 2020: deaths by cause, age, sex, by country and by region, 2000–2019 [Internet]. Geneva: WHO; 2020 [cited 2025 Jan 10]. Available from: https://www.who.int/data/gho/data/themes/mortality-and-global-health-estimates
3. Cornford P, van den Bergh RCN, Briers E, Van den Broeck T, Cumberbatch MG, De Santis M, et al. EAU-EANM-ESTRO-ESUR-SIOG Guidelines on Prostate Cancer. Part II—2020 Update: Treatment of Relapsing and Metastatic Prostate Cancer. European Urology. 2021;79(2):263–82.
4. Hofman MS, Emmett L, Sandhu S, Iravani A, Joshua AM, Goh JC, et al. [177Lu]Lu-PSMA-617 versus cabazitaxel in patients with metastatic castration-resistant prostate cancer (TheraP): a randomised, open-label, phase 2 trial. Lancet. 2021;397(10276):797–804.
5. Sartor O, de Bono J, Chi KN, Fizazi K, Herrmann K, Rahbar K, et al. Lutetium-177-PSMA-617 for metastatic castration-resistant prostate cancer. N Engl J Med. 2021;385(12):1091–103.
6. Fendler WP, Calais J, Eiber M, Flavell RR, Mishoe A, Feng FY, et al. Assessment of 68Ga-PSMA-11 PET accuracy in localizing recurrent prostate cancer: a prospective single-arm clinical trial. JAMA Oncol. 2019;5(6):856–63.
7. Uprimny C, Kroiss AS, Decristoforo C, Fritz J, von Guggenberg E, Kendler D, Scarpa L, Di Santo G, Roig LG, Maffey-Steffan J, Horninger W. 68Ga-PSMA-11 PET/CT in primary staging of prostate cancer: PSA and Gleason score predict the intensity of tracer accumulation in the primary tumour. European journal of nuclear medicine and molecular imaging. 2017 Jun;44(6):941-9.
8. Giesel FL, Hadaschik B, Cardinale J, Radtke J, Vinsensia M, Lehnert W, Kesch C, Tolstov Y, Singer S, Grabe N, Duensing S. F-18 labelled PSMA-1007: biodistribution, radiation dosimetry and histopathological validation of tumor lesions in prostate cancer patients. European journal of nuclear medicine and molecular imaging. 2017 Apr;44(4):678-88.
9. Warburg O. On the origin of cancer cells. Science. 1956 Feb 24;123(3191):309-14.
10. Jadvar H. Is there use for FDG-PET in prostate cancer?. InSeminars in nuclear medicine 2016

    Nov 1 (Vol. 46, No. 6, pp. 502-506). WB Saunders.
11. Beauregard JM, Blouin AC, Fradet V, Caron A, Fradet Y, Lemay C, et al. FDG-PET/CT for pre-operative staging and post-operative restaging of prostate cancer. Eur J Nucl Med Mol Imaging. 2015;42(11):1670–9.
12. Aggarwal R, Wei X, Kim W, Small EJ, Ryan CJ, Carroll P, et al. Heterogeneous fluciclovine and PSMA-ligand PET uptake in metastatic prostate cancer: a proof of concept study. Eur J Nucl Med Mol Imaging. 2021;48(6):1903–13.

13. Hope TA, Aggarwal R, Chee B, Tao D, Greene KL, Cooperberg MR, Feng F, Chang A, Ryan CJ, Small EJ, Carroll PR. Impact of 68Ga-PSMA-11 PET on management in patients with biochemically recurrent prostate cancer. Journal of Nuclear Medicine. 2017 Dec 1;58(12):1956-61.

14. Pyka T, Okamoto S, Dahlbender M, Tauber R, Retz M, Heck M, Tamaki N, Schwaiger M, Maurer T, Eiber M. Comparison of bone scintigraphy and 68Ga-PSMA PET for skeletal staging in prostate cancer. European journal of nuclear medicine and molecular imaging. 2016 Nov;43(12):2114-21.

15. Bakht MK, Derecichei I, Li Y, Ferraiuolo RM, Dunning M, Oh SW, Hussein A, Youn H, Stringer KF, Jeong CW, Cheon GJ. Neuroendocrine differentiation of prostate cancer leads to PSMA suppression. Endocrine-related cancer. 2019 Feb 1;26(2):131-46.

16. Zeigler-Johnson CM, Tierney A, Rebbeck TR, Rundle A. Prostate cancer severity associations with neighborhood deprivation. Prostate Cancer. 2011;2011(1):846263.